Climate Dynamics

Two key parameters for the El Nino continuum: zonal wind anomalies and Western Pacific subsurface potential temperature

--Manuscript Draft--

Manuscript Number:	CLDY-D-14-00665R1
Full Title:	Two key parameters for the El Nino continuum: zonal wind anomalies and Western Pacific subsurface potential temperature
Article Type:	Original Article
Keywords:	Central Pacific El Niño; El Niño continuum; Zonal wind anomalies; Oceanic potential temperature; Thermocline discharge-recharge state
Corresponding Author:	Andy Wang-Chun Lai, BSc, MPhil, ARCS, ATCL University of Cambridge Cambridge, UNITED KINGDOM
Corresponding Author Secondary Information:	
Corresponding Author's Institution:	University of Cambridge
Corresponding Author's Secondary Institution:	
First Author:	Andy Wang-Chun Lai, BSc, MPhil, ARCS, ATCL
First Author Secondary Information:	
Order of Authors:	Andy Wang-Chun Lai, BSc, MPhil, ARCS, ATCL
	Michael Herzog, MSc, PhD
	Hans Friedrich Graf, MSc, PhD, DrSc
Order of Authors Secondary Information:	
Abstract:	Different types of El Niño (EN) events have recently been discussed. Based on NCEP-NOAA reanalysis data this analysis explores a number of key parameters that cause a range of EN types over the period 1980-2013. EN events are divided into three types depending on the spatial and temporal evolution of the sea surface temperature anomalies (SSTA): Central Pacific (CPEN), Eastern Pacific (EPEN), and Hybrid (HBEN). We find that EN is a continuous spectrum of events with CPEN and EPEN as the end members. This spectrum mainly depends on two key parameters: the 130ºE-160ºE Western Pacific 5m-250m subsurface oceanic potential temperature anomaly (PTA) about one year before the EN peak (typically January and February), and the 140ºE-160ºW cumulative zonal wind anomaly (ZWA) between onset and peak of the EN event. Using these two parameters, about 70% of the total variance of the maximum SSTA realised in different Niño regions can already be explained up to six months before the maximum SSTA occurs. This offers a rather simple potential for ENSO prediction. A necessary condition for the evolution of an EPEN, the Western Pacific is in the recharged state. Strong and sustained westerly wind anomalies in Western Pacific can then trigger a Kelvin wave propagating to the eastern Pacific. Both parameters, potential temperature and zonal wind anomaly, constructively interfere. For a CPEN, these parameters are much less important. Kelvin wave propagation is not involved in the evolution of the event. Instead, the Central Pacific warming is caused locally by a zonal advection feedback and local air-sea interaction as already demonstrated in previous studies. The HBEN occurs when both parameters interfere in different ways: (1) Western Pacific is weakly charged, but strong westerly ZWA are observed that reduce the equatorial upwelling in the Central Pacific while the triggered Kelvin wave is too weak to have a significant effect; (2) Western Pacific is strongly charged but only weak westerly ZWA develop, so that the resulting Kelvin wave cannot fully extend into the eastern-most Pacific.

Two key parameters for the El Niño continuum: Zonal wind anomalies and Western Pacific subsurface potential temperature

ANDY WANG-CHUN LAI[1*]

MICHAEL HERZOG[1]

HANS-F. GRAF[1]

[1]*Centre for Atmospheric Science, University of Cambridge, Downing Place, Cambridge CB2 3EN, UK*

**Corresponding author: wcal2@cam.ac.uk*

Abstract

Different types of El Niño (EN) events have recently been discussed. Based on NCEP-NOAA reanalysis data this analysis explores a number of key parameters that cause a range of EN types over the period 1980-2013. EN events are divided into three types depending on the spatial and temporal evolution of the sea surface temperature anomalies (SSTA): Central Pacific (CPEN), Eastern Pacific (EPEN), and Hybrid (HBEN). We find that EN is a continuous spectrum of events with CPEN and EPEN as the end members. This spectrum mainly depends on two key parameters: the 130ºE-160ºE Western Pacific 5m-250m subsurface oceanic potential temperature anomaly (PTA) about one year before the EN peak (typically January and February), and the 140ºE-160ºW cumulative zonal wind anomaly (ZWA) between onset and peak of the EN event. Using these two parameters, about 70% of the total variance of the maximum SSTA realised in different Niño regions can already be explained up to six months before the maximum SSTA occurs. This offers a rather simple potential for ENSO prediction.

A necessary condition for the evolution of an EPEN, the Western Pacific is in the recharged state. Strong and sustained westerly wind anomalies in Western Pacific can then trigger a Kelvin wave propagating to the eastern Pacific. Both parameters, potential temperature and zonal wind anomaly, constructively interfere. For a CPEN, these parameters are much less important. Kelvin wave propagation is not involved in the evolution of the event. Instead, the Central Pacific warming is caused locally by a zonal advection feedback and local air-sea interaction as already demonstrated in previous studies. The HBEN occurs when both parameters interfere in different ways: (1) Western Pacific is weakly charged, but strong westerly ZWA are observed that reduce the equatorial upwelling in the Central Pacific while the triggered Kelvin wave is too weak to have a significant effect; (2) Western Pacific is strongly charged but only weak westerly ZWA develop, so that the resulting Kelvin wave cannot fully extend into the eastern-most Pacific.

Keywords:

Central Pacific El Niño • El Niño continuum • Zonal wind anomalies • Oceanic potential temperature • Thermocline discharge-recharge state

38

1. Introduction

40 El Niño (EN) is the warm phase of the oceanic component of the dominant mode of interannual tropical climate variability called El Niño-Southern Oscillation (ENSO) occurring every 3 to 5 years. This
42 phenomenon has attracted continuous scientific and public interest for decades because it has significant global climatic teleconnections and is the most dominant feature of tropical climate variability on sub-decadal
44 timescales.

The canonical Eastern Pacific EN (EPEN) refers to a band of anomalously warm equatorial ocean
46 water temperatures that develop off the western coast of South America into the equatorial Pacific. Recently, there have been numerous reports on a "new" type of EN, the Central Pacific El Niño (CPEN) (Ashok et al.
48 2007; Kao and Yu 2009; Yeh et al. 2009). It is characterized by predominantly positive sea surface temperature anomalies in the tropical Central Pacific (CP) rather than in the East Pacific (EP). The two EN types have
50 different teleconnections and climatic impacts (Ashok et al. 2007; Kao and Yu 2009; Kug et al. 2009; Yu and Kim 2010, Graf and Zanchettin 2012). Although there are some well accepted hypotheses for the development
52 of the ENSO, the actual triggering mechanism is still debated. For example, one perspective is that evolution of ENSO is largely controlled by self-sustaining oscillatory internal dynamics rather than by stochastic forcing (Jin
54 1999; Chen et al. 2004). Another view is that ENSOs are in fact event-like disturbances on top of a stable basic state, requiring an initiating trigger not contained in the dynamics of the cycle itself (Kessler 2002). However, as
56 seen in observations, every EN has a different characteristic and, hence, EN can be seen as a continuous spectrum of events, a so-called "El Nino continuum", rather than well defined patterns (Giese and Ray 2011).
58 Johnson (2013) statistically explored different EN flavours and identified four types for the ENSO warm phase (Fig 2 in Johnson, 2013), with cluster patterns "6" and "7" in his study illustrating CPEN pattern. However, he
60 concludes that the central longitude of the EN sea surface temperature anomalies (SSTA) is not bimodal, and is indistinguishable from a Gaussian distribution centred near 140ºW. Yet, there are other studies suggesting that
62 CPEN should be classified as a separate ENSO type. Ashok et al. (2007) and Pascolini-Campbell et al. (2014) have demonstrated that the currently used indices for identifying ENSO are too simplistic and do not fully
64 capture EN types in the past.

Low-frequency climatic variability could play a role in the occurrence of different EN types. Seasonal
66 footprinting mechanisms linked to the state of the North Pacific Oscillation (NPO) (Vimont et al. 2001, 2003) are explored in Chen et al. (2013). Their study concluded that an ENSO event would not necessarily occur under
68 a positive NPO. Only if a positive wintertime NPO coincides with a positive phase of the Arctic Oscillation in spring, a significant ENSO-like warming anomaly will occur in the following winter. A recent study by Hong et
70 al. (2013) suggests there is a climate regime shift in the Pacific SST anomaly pattern around 1996-97. Warming over the equatorial WP and cooling over the CP is probably responsible for the strengthened trade winds
72 reported in the study by England et al. (2014). This may be a consequence of the warming that started earlier over the Indian Ocean (Rao et al. 2011).

74 Although the existence of different EN types has only received attention quite recently, already Graf (1986) discussed possible mechanisms associated with two different types of EN, CPEN and EPEN, and how
76 they might be linked (Figure 1). In general, positive SSTA in EP or CP may be caused by a decrease in trade winds and Western Pacific westerly wind anomalies. Westerly wind anomalies may be caused by tropical or
78 extratopical drivers. Extratropical drivers include seasonal high latitude warming in boreal summer weakening the general circulation by a decrease in the meridional temperature gradient that leads to weaker trade winds
80 (Graf 1986; Vecchi et al. 2006). Tropical drivers that may cause an increase in westerly wind anomalies include the Madden-Julian Oscillation (MJO). During the early phase of the MJO, the Western Pacific is cooled due to
82 increased cloud cover while the CP remains warm. Subsequently, convective activity migrates from the Western Pacific into the CP. The accompanying westerly surface wind anomalies promote further CP warming (Bergman

et al. 2000). Cold air outbreaks from the Asian winter monsoon also may generate westerly wind bursts with consequences for the triggering of equatorial Kelvin waves (e.g. Graf, 1986, Chen et al., 2013).

The canonical EPEN is characterized by basin-wide thermocline variations in the zonal direction of the equatorial Pacific. Under neutral conditions, easterly trade winds contribute to the accumulation of warm water in the Western Pacific (WP) building up potential temperature anomalies while deepening the thermocline. EPEN follows the delayed-oscillator theory of ENSO (Suarez and Schopf, 1988; Battisti and Hirst, 1989), with an effective discharge of water mass and thermal energy (Jin 1997). Therefore, typically an EPEN episode will be followed by a La Niña. Thus, the EP type ENSO evokes a phase-reversal signal and behaves like a damped oscillation. The warm water masses piled up in the WP warm pool can propagate as an oceanic Kelvin wave from the WP to the EP. This Kelvin wave can be triggered by an anomalously weak Walker circulation, by anomalously weak trade winds, or by westerly wind bursts over the west and central Pacific. Triggering mechanisms can originate from cold air outbreaks of the Asian winter monsoon or from transient disturbances induced from strong MJO events (Graf 1986; Fedorov 2002; McPhaden et al. 2006). The Kelvin wave mechanism plays a major role in generating positive SSTA over the EP by the thermocline feedback, where the change in thermocline depth leads to the SST change through modifying the upwelled subsurface property (Jin and An, 1999).

For the evolution of a CPEN the role of thermocline variations is limited. CPEN is much more related to local atmospheric forcing. It is usually triggered by a moderately weakened trade wind and some westerly wind anomalies resulting in wind convergence from either side of the Pacific over the CP (Graf 1986; Ashok et al. 2007). This leads to zonal oceanic current anomalies inducing positive SSTA through zonal advection. Positive SSTA, via their effect on deep convection, in turn induce additional surface wind anomalies further strengthening this SSTA in a “zonal advection feedback” (Yeh et al. 2014). A further positive feedback is resulting from the “latent heat feedback”, whereby the westerly wind anomalies (i.e. weaker easterly winds) caused by the existing positive SSTA and their effect on convective activity reduce the latent heat release from the ocean surface leading to further CP warming. The associated surface wind anomalies and SSTA tend to onset, develop, and decay in situ, and do not have a phase-reversal signal. CP type ENSOs behave like local events rather than as part of a cycle (for observations see Kao and Yu (2008), for models see Guilyardi (2006) and Guilyardi et al. (2009)).

Graf (1986) also suggests that CPEN can be a precursor of an EPEN. The initial CP warming shifts the convective activity from the WP warm pool eastwards and induces westerly wind anomalies over the WP warm pool, which, if strong enough, can trigger a Kelvin wave if a potential temperature anomaly (i.e. deep thermocline, warm water piled up in the warm pool) has been previously established. Such a Kelvin wave would propagate eastward along the equator near the depth of the thermocline. While the CP warming is maintained locally, an EPEN starts due to this thermocline feedback. As soon as the Kelvin wave reaches the far Eastern Pacific the thermocline there is deepened and SST increases. These positive SSTA then extend westwards and unite with the pre-existing CP warm surface waters. Such an event may be called “Hybrid El Niño” (HBEN). Figure 1, adopted and simplified from Graf (1986), illustrates these atmospheric and oceanic pathways leading to the different types of EN. Schneider et al. (1995) shows that westward propagating off-equatorial (around 5ºN/S) heat content anomalies in the WP are excited by wind stress forcing near the CP. These Rossby waves can determine the WP recharged state and the potential for Kelvin waves.

Recent studies by Fedorov et al. (2014) and Hu et al. (2014) explored the diversity of EN types that are potentially caused by the effect of a westerly wind burst (WWB) on the ocean in a recharged state. These modelling studies prescribed a one-month WWB to various different oceanic recharged states. Different strength of the recharged states and WWB can result in EPEN or CPEN. We will explore this in more detail using observations to validate and extend their findings.

The above discussion suggests that the analysis of EN events should not be static, but cover the evolution of individual events. We will therefore investigate the temporal evolution of EN events from available

oceanic observations and atmospheric reanalysis data. The results will show that a few key parameters are sufficient to statistically represent the EN continuum and that CPEN and EPEN are the end members of this continuum.

2. Methodology and Data

2.1 Datasets

The datasets used in this study include monthly mean SSTA, oceanic subsurface potential temperature, oceanic 20ºC isothermal depth, and zonal wind at 10m altitude.

The SSTA was obtained from the National Centres for Environmental Prediction, National Oceanic and Atmospheric Administration (NCEP/NOAA) reanalysis (Reynolds et al. 2002) version 2 with 1º x 1º horizontal resolution. Its SST fields were updated from version 1 with more data from the Comprehensive Ocean-Atmosphere Data Set (COADS), and with a new sea-ice to SST conversion algorithm.

The upper ocean heat content can be estimated by different parameters (e.g. Meinen and McPhaden 2000; Fedorov et al. 2014). We have chosen to use the ocean 20ºC isothermal depth and oceanic potential temperature as a function of depth obtained from the Behringer et al. (2004) Global Ocean Data Assimilation System (GODAS). They represent the ocean heat content without further calculation, and can be obtained directly from GODAS.

The NOAA NCEP Reanalysis 2 was used for zonal wind since it is based on an improved model with updated parameterisations of physical processes compared to NOAA NCEP reanalysis 1 and includes more observations (Compo et al. 2011). The ERA-Interim zonal wind reanalysis from the European Centre for Medium Range Weather Forecast has amplitudes of the anomalies and spatial patterns similar to the NOAA NCEP reanalysis.

Since data before 1980 are not available for the GODAS datasets, all studies are conducted for the 1980 to 2013 period. All variables presented here are based on monthly means. Anomalies are deviations from the 1981 to 2010 climatology.

2.2 Characterisation of El Niño events

There has been a lot of discussion about different types of El Niño in the recent past. While some authors advocate for the differentiation between CPEN and EPEN (Ashok et al. 2007; Kao and Yu 2009; Kug et al. 2009), others claim EN to be a continuum thus making a classification rather useless (Giese and Ray 2011). Most of the classifications are done statically, based on classical ENSO indices. Only few authors used pattern analysis (Johnsons 2013). Here we go beyond previous attempts by analysing the evolution of SSTA pattern for individual EN events. . In line with our main conclusion of an EN continuum we do not attempt to classify but rather characterise EN events.

We define the beginning of an ENSO cycle when SSTA average for at least six consecutive months exceeds +0.5K anywhere between 160ºE to 80ºW along the 5ºN-5ºS equatorial band. The onset month is the first month of the six consecutive months. Compared with the NOAA CDC classification, our analysis extends the region of analysis to the whole equatorial Pacific covering the Niño4 to Niño1+2 regions. The end of an ENSO event is marked by the month in which the SSTA drops again below +0.5K and SSTA stay below +0.5K for at least three more months in the 160ºE-80ºW, 5ºN-5ºS region. It would be a new ENSO event if the threshold were exceeded afterwards.

During an ENSO event, monthly SSTA patterns are analysed. A monthly pattern is considered a CP warming pattern if the SSTA of 1.0K or above do not reach the coast of Peru (Niño-1+2 region). The threshold

of 1.0K is chosen because 0.5K threshold (used for defining onset and end of the ENSO episode) is not sufficiently high enough to distinguish the spatial differences between CPEN and EPEN. The 0.5K signals are noisy over the cold tongue. The 1.0K threshold ensures the detection of signals are above the noise.

An EP positive SSTA pattern has maximum SSTA of 1.0K or above near the coast of Peru (or the Niño-1+2). Using this pattern analysis, we can describe the temporal evolution of individual EN events.

An EN event is considered to be a CPEN event if only the CP warming pattern occurs during its evolution. It is considered an EPEN event if more months are characterized by an EPEN than CPEN pattern over the lifetime of the event. Mixed CP and EP warming patterns occurring over the lifetime simultaneously or subsequently will be called Hybrid El Niño events (HBEN). As it will turn out, ENSOs can be seen as a continuum with the end members being CPEN and EPEN events.

Our method is unique and differs slightly from other studies that attempted to classify different EN types, because we have introduced an HBEN. Pascolini-Campbell et al. (2014) explicitly explored various different studies that attempted to classify EN events, and found that different methods and datasets yield different results. They also emphasise that solely relying on indices may lead to misclassifications. Many methodologies only use traditional ENSO indices (e.g. Ashok et al. 2007), empirical orthogonal function (EOF) (e.g. Takahashi et al. 2011; Yu and Kim 2012), or composites of the boreal winter (e.g. Yeh et al. 2009). These are static and do not capture the temporal evolution of patterns. Lian and Chen (2012) also raise doubts on classification of SST variability using EOFs. Therefore, it is not surprising that some events that were classified as CPENs in previous studies actually show a HBEN characteristic when the temporal evolution of patterns is taken into account.

3. Results

3.1. The identified El Niño events

The analysis of SST data since 1980 allows identifying 10 El Niño episodes with different characteristics as presented in Table 1. The identified types of El Niños match previous classifications by Johnson (2013). CPEN is equivalent to Johnson's (2013) cluster pattern "6" and "7", HBEP and EPEN are number "8" and "9", respectively - see figures 2 and 3 in Johnson (2013). The methodology used here adds more information about the evolution of an EN event, whereas in Johnson (2013), only the ENSO peak period [Sep(0)-Feb(1)] is used and thus the pattern evolution is not considered. Time notations (-1), (0), and (1) indicate the year before, during, and after the EN occurrence, respectively. The information provided in Table 1 shows that the CP SSTA pattern is present for all ENSO events. The CP warming pattern forms an integral part of any ENSO evolution and, consistent with the hypothesis of Graf (1986), almost all ENSO episodes started with a CP SSTA pattern. The two exceptions (2009-10, 2006-07) started with simultaneous CP & EP SSTA patterns. All CPEN and HBEN cases ended with a CP warming pattern, whereas the EPEN (1982-83 and 1997-98) SSTA patterns were retained until they turned into La Niña conditions without shifting back to a positive CP SSTA pattern. The EPEN type is the strongest EN, with maximum SSTA almost 3ºC higher than for all other EN. Conversely, CPEN is always a weaker EN event in terms of SSTA. Its maximum SSTA never exceeded 2ºC. However, we have to keep in mind that the location of these weaker SSTA in the central equatorial Pacific are on top of an already warm climatological SSTA and, thus, may lead to stronger precipitation anomalies and teleconnections (Graf and Zanchettin, 2012).

According to table 1 the dominant ENSO flavour is HB of which there were six, in addition to only two CPEN, and two EPEN. This result is consistent with (Newman et al. 2011) who claim that ENSO events form a continuum of mixed CP & EP patterns. Even though a HB classification is not mentioned in their study, their results imply that HB should be the common pattern. Both EPEN are preceded by CP warming. This can be understood since enhanced convection over the CP leads to westerly wind anomalies over the WP that can

trigger a Kelvin wave that potentially leads to an EPEN (Graf 1986). Another important difference between different EN events is the month of the first significant SSTA anomaly, which is in boreal spring (March/April) for EP events, but later in the year (between May and September) for all other events

Having defined the individual EN events and their types based on the evolution of SSTA patterns, we will now investigate some of the relevant oceanic and atmospheric parameters that determine the evolution of EN episodes. We will concentrate here on oceanic subsurface potential temperature and atmospheric zonal wind anomalies since these are the most important parameters for equatorial Kelvin waves that play a central role in EN dynamics (Graf 1986; Jin 1997; Jin and An 1999; Chen et al. 2013).

3.2. Oceanic subsurface potential temperature and Kelvin waves

The oceanic potential temperature anomalies (PTA) as a function of depth was analysed, which allows a better understanding of the role of oceanic dynamics in different ENSO types than just SSTA. The potential temperature is the temperature that a parcel of water would have if it were moved adiabatically to a reference pressure. This means the effective temperature after removing the heat of the parcel associated solely with compression. Reference pressure is the ocean surface, with water pressure at zero decibar (Baum 2001). Potential temperature instead of in-situ temperature is used so that the heat content of water masses can be compared across different depths. In **Figure 2** PTA are displayed across the equatorial Pacific next to the patterns of SSTA for the different stages of all individual EN episodes. The Figure is organised by EN types as defined in Table 1: EPEN (2a), CPEN (2b) and HBEN (2c). We have introduced a simple significance test based on 1.3 Sigma indicating a 80% confidence level based on a two-tailed z-test. Areas with anomalies exceeding the 1.3 Sigma level are hatched in **Figure 2**. The calculated sigma is a conservative estimate since it includes the variability produced by El Nino and La Nina events.

The left-most panels in **Figure 2** display the two-month averages of PTA before the onset of ENSO (as defined in Table 1). Positive PTA in the WP region of 130ºE-170ºE indicate that the equatorial ocean there is "loaded" corresponding to a recharged thermocline state in terms of the recharge-discharge oscillator (Jin 1997). The columns following to the right are for the months associated with the onset, peak, and end of the ENSO event, respectively. The corresponding SSTA plots are shown below the PTA analysis. The Hovmoller diagrams of the PTA and the 20ºC isothermal depth (thereafter called isothermal depth) in **Figure 3** are plotted for the 1997-98 EPEN, the 2004-05 CPEN, and the 2009-10 HBEN. These examples are selected because they are the best representation of some distinctive features seen below the ocean surface for each ENSO type.

For the Western Pacific recharged state, we considered the PTA average over the volume of 5ºN-5ºS, 130ºE-160ºE, and the top 250m. Stronger recharged states are characterised by larger positive PTA. When considering the PTA across the equatorial Pacific, the depth and strength of positive PTA increases from CPEN, HB, to EPEN for the onset and peak of the ENSO events, although there are significant differences between individual events. EPEN shows an extensive basin-wide phenomenon of large West-East anomalies of opposite signs during its peak, whereas CPEN exhibits a more local subsurface temperature evolution over the CP, and HBEN shows a combination of both features.

The observed positive PTA in EPEN (**Figure 2a**) is a downwelling Kelvin wave. Its propagation is shown in **Figure 3a**. Left panels of **Figure 2a** show the months before the onset of EPEN. The WP region is filled with positive PTA to a depth of about 250m, indicating a recharged state. At the beginning of the EPEN, while there are SSTA near the CP and off-equatorial CP, the positive PTA starts to propagate as a Kelvin wave toward the EP (also shown in **Figure** 3a) and the SSTA moves slightly to the East as well. The EPEN starts off with a CP warming and the Kelvin wave is propagating underneath the CP warm anomalies at the thermocline depth with rather weaker effects on the SSTA. During the peak of EPEN, the Kelvin wave has propagated to the EP, causing positive PTA reaching the ocean surface and covering the entire EP (180º-90ºW). In addition, positive PTA penetrate to a depth of up to 350m. This process manifests itself in a strong EP SSTA signal.

During this peak period, a large out-of-phase anomaly is seen: negative PTA appear over the WP. These negative PTA are the upwelling Kelvin waves during the EPEN decay phase and will eventually reverse the phase of ENSO into La Niña. This is the typical phase-transition mechanism of an EPEN. The upwelling Kelvin wave is originating from the reflection of Rossby waves over the WP. This is consistent with the delayed-oscillator theory (Suarez and Schopf, 1988; Battisti and Hirst, 1989; Kug et al. 2009).

In the two CPEN cases of 2003/4 and 2004/5 the WP is not recharged before the onset of the event. The overall growth of the positive PTA is localised over the CP region. During the peak of the CPEN, when SSTA reach their largest extent over the CP, deep penetration and propagation of the PTA, as typical for EPEN, is not observed (**Figure 2b**). Over time, the positive PTA near 180º spread across the ocean subsurface in zonal direction and decay. The fact that the WP is not in a recharged state implies a weak potential for Kelvin wave propagation.

The HBEN cases show features and magnitudes between that of the CPEN and EPEN with high variability. They have onsets like a weak CPEN (except 2009-10), with a surface warming around 160-180ºE, also apparent in the SSTA (**Figure 2c**). Positive PTA is seen two months before the onset and in the onset month at the subsurface down to a depth of about 200m. An eastward propagating Kelvin wave like in the EPEN case is observed (see also **Figure 3c**), but with smaller amplitude and high variability between the individual cases. At the peak of the HBEN, the EPEN-like PTA patterns are evident: positive PTA from 180º to 80ºW and negative PTA to the West, but again, with smaller amplitude than for EPEN. The Kelvin wave induced deepening of the thermocline leads to an EPEN-like pattern at the surface (second right panel, **Figure 2c**). The out-of-phase PTA signal is observed at the end of the event similar to EPEN. The upwelling Kelvin wave then propagates eastward during the decay phase, potentially leading to an ENSO reversal. However, the CP SSTA and a shallow subsurface (50m) warming remain when the EPEN pattern disappears.

Considering only the WP recharged state does not fully explain why some events evolve into an EPEN, and some only evolve into a moderate HBEN. In the 1994-95 event, for example, the analysis of **Figure 2c** and 20ºC isothermal depth anomalies (not shown) reveals that the WP region was at a discharged state at the onset when a CP warming started in July 1994. This CP warming intensified, leading to a deepening of the thermocline locally in the CP. This was then deep enough to create the potential for the observed Kelvin wave propagating eastward from the CP. In contrast, during the 2002-03 HBEN event the WP was in a recharged state, but had similar maximum SSTA (2.9ºC) compared to the 1994-95 HBEN event (2.7ºC).

For the EPEN cases, a recharged state of the WP before the main EN event is necessary to create the potential for a Kelvin wave that can travel eastward underneath an initial CP warming. This can also happen for the HBEN cases. When this happens, it leads to an EP warming pattern. For HBEN and EPEN a negative PTA region is also observed to the west of the Kelvin wave towards the end of the ENSO cycle. This is consistent with the delayed oscillator theory and indicates the phase reversal due to thermocline variations that can lead to a La Niña episode in the following year. For HBEN events the amplitude of the PTA variations are smaller. Each HBEN could become a fully-fledged EPEN event, but either the Kelvin wave is not travelling far enough into the EP or is not strong enough.

For EPEN, **Figure 3a** highlights the clear eastward propagation of a sequence of Kelvin waves, indicated by the arrows according to the overall PTA and isothermal depth patterns, and the monthly maximum PTA (shown in dots). When the Kelvin wave at the thermocline depth reaches 90ºW (e.g. middle panel in Figure 3a), the near surface water east of 180º (EP) warms up as the anomalously warm water is formed near the surface by the thermocline feedback over the EP. This near surface warming reaches into the CP near 180º where it persists until Apr-1997. The Western Pacific region (west of 180º) is at a recharged state (middle panel, **Figure 3a**) before the onset of the EN event and before the propagation. The 2009-10 HBEN (**Figure 3c**) has patterns like the EPEN but with smaller magnitude during the eastward propagation of the positive PTA. Note that the Western Pacific recharged state for this HBEN is very pronounced and even slightly stronger than for the 1997-98 EPEN. For the CPEN, very weak or no propagation is seen at both depths (**Figure 3b**) as indicated

by the near straight vertical pattern. **Figure 3b** also includes the 2003-04 CPEN, which has a similar pattern as 2004-05. The positive PTA grows locally at all depths over the CP region of Niño-4, implying that no Kelvin wave is involved. The western-most Pacific region is not recharged before the onset.

In **Figure 4** the maximum change in the 20ºC isothermal depth that occurred during an EN event over the EP region at 100ºW is plotted against the maximum SSTA anywhere between 160ºE-80ºW. The 20ºC isothermal depth is a common proxy used by NOAA for the variations in the thermocline and detection of Kelvin waves. The 100ºW maximum change in the 20ºC isothermal depth and the maximum SSTA correlate linearly very well with explained variance R^2 = 0.88. The graph is an illustration of how the ENSO intensity varies with ENSO types, and also indicates the importance of the thermocline feedback. The more EPEN-like the event is, the larger the maximum SSTA, and the stronger the thermocline depth variation due to a stronger Kelvin wave. As the debates on different ENSO types continue, this graph illustrates that the three ENSO types are separated into three distinct clusters, but also that there is still a continuum with EPEN and CPEN as clear end members. The continuum is caused by variations in strength of the Kelvin waves and the longitudinal extents to which they can propagate. Without large isothermal depth anomalies (IDA), there is weak potential for Kelvin waves. The CP air-sea interactions only lead to a relatively weak and local anomalous CP warming. Yet, when the IDA is strong, a deep WP/CP thermocline (right panels, **Figure 3**) can favour the excitation of a significant Kelvin waves strongly influencing the EP SST through the thermocline feedback generating a strong and immediate warming over the EP (Jin and An 1999; An and Jin 2001; Kug et al. 2009).

Different EN characteristics are associated with the extent to which the thermocline feedback affects the SST. Eastward propagating Kelvin waves play a key role in warming the EP. Weaker Kelvin waves can lead to HBEN, with SSTA smaller than during EPEN. No thermocline feedback mechanism is involved for the CPEN, and SSTA are weakest. The amplitude of the SSTA over the EP that depend on the thermocline feedback form a continuum across EN events.

3.3 Western Pacific recharged state

Since the WP recharged thermocline state is one of the essential factors in determining the ENSO evolution as discussed in section 3.2, we show in **Figure 5** top panel the time series of volume mean PTA over the WP (140ºE-170ºE, 5ºN-5ºS, 5m-250m) for each ENSO event, and for the composites of each ENSO type (bottom panel, **Figure 5**). The lines are colour coded: green, grey, and red correspond to CPEN, HBEN, and EPEN respectively.

Each EN event behaves differently creating a strong variability, especially in the HB class. However, there are still a number of common and distinctive features. While most of the events show a recharged WP state indicated by the positive PTA during the winter before the event, this is not the case for two events (CP 2003/04 and HB 1994/95). The composite plot (**Figure 5** bottom panel) shows a clearer picture and resembles the observations in section 3.2, but we must keep in mind that the variability is strong, for instance, up to +/– 1.2K for HBEN and +/– 0.8K for CPEN, so other factors apart from the recharged state are affecting the ENSO evolution. In the mean over the two events, EPEN shows the strongest recharged state almost a year before the peak of the event. The PTA drops significantly to negative values and reaches its minimum around Dec(0) for the EPEN. This indicates the westward propagating Rossby wave has reached the WP region and turning into an upwelling Kelvin wave at the peak of the EN event as shown by the strong eastward propagating negative PTA in **Figures 2a and 3a**. Oceanic Kelvin and Rossby waves, which propagate in opposite directions, are forced by the basin boundaries to change into opposite wave characteristics through reflections (Suarez and Schopf, 1988; Jin 1997; Kug et al. 2009). The large amplitude also shows the strong phase-reversal signal of a typical EPEN. The CPEN case shows a very different behaviour. PTA were below 0.5K before May(0) indicating the lack of a recharged state (Hu et al. 2014), and therefore no phase-reversal mechanism is involved as shown by the relatively flat signal. In the mean HBEN shows features somewhere between the two end members: moderately recharged and phase-reversed with large variations between individual cases. The recharged states prior to HB

are generally weaker than before the two EPEN events before May(0), except for 2006-07 and 2009-10. These two most recent events behave quite similar in time. It is interesting to note that the recharged state of the 1986-87 HBEN early in the year was comparable to the 1982-83 EPEN. Both events start with a high positive PTA, but the phase reversal is limited. Obviously the strength of positive PTA alone is not sufficient to generate a really strong EN event.

For completeness, the 130ºE-160ºE x 5ºN-5ºS mean 20ºC isothermal depth is displayed in **Figure 6**. Generally, a stronger positive PTA is reflected by a deeper thermocline. Both parameters are highly correlated with a joint variability of $R^2 = 0.84$.

The isothermal depth composites in **Figure 6** (bottom panel) show that in the EPEN case the thermocline is initially deeper, confirming the recharged state. HBEN shows values in between that of the CP and EPEN, and highly variable conditions as shown in top panel of **Figure 6**. Once again, the events in 2006-07 and 2009-10 show slightly deeper isothermal depth than the EPEN events around Feb(0). In section 3.5 we will discuss why some strongly WP recharged states early in the year did not result in a EPEN-like event.

The CPEN shows a shallower thermocline depth and flatter profile after boreal spring, confirming the absence of a potential for a significant Kelvin wave. Several studies have shown that the associated CP SSTA are caused by sea-air interaction and zonal advection feedback (Ashok et al. 2007; Kao et al. 2009; Kug et al. 2009). The zonal SST gradient is strong due to the WP warm pool and EP cold tongue. Equatorial zonal ocean current anomalies can induce SSTA through zonal advection, and in turn induce zonal wind anomalies. The westerly wind anomalies over the WP and easterlies over the EP lead to surface convergence over the CP. The westerlies enhance SST warming by reduced equatorial upwelling, and the easterlies suppress the warming over the EP by enhanced upwelling.

A plot similar to **Figure 4** is produced in **Figure 7**, but for the WP 140ºE-160ºE region. As for the EP region in **Figure 4**, a continuum is observed for the three EN types like in **Figure 2**, but the correlation is less strong, with $R^2 = 0.55$ (0.88 for EP in **Figure 4**). **Figure 7** shows that for CPEN, a small change in the thermocline depth in the WP implies that no discharge process can take place and there is little potential for a Kelvin wave to propagate eastwards. The anomalies remain local. Although HBEN and EPEN have a similar change in the WP thermocline depth in the West Pacific, they develop distinctively different maximum SSTA in the East Pacific.

To summarize, the WP about a year before an EPENs was in a thermocline-recharged state, suggesting a strong potential for major Kelvin waves to propagate east. For CPEN, the WP was not recharged, supporting the fact that no Kelvin wave was involved. For some HBENs, recharged states were as strong as for the EPENs, and were weaker for the other HBENs. The different recharged states that have led to similar intensities suggest that other factors were involved in the EN evolution. We will next analyze the equatorial zonal wind anomalies as a potential parameter creating these East Pacific SSTA differences.

3.4 Zonal wind anomalies

Figure 8 shows time series for the WP to CP cumulative 10m zonal wind anomalies covering 140ºE-160ºW (ZWA), accumulated from Nov(-1) to the indicated month. In a given month, positive (negative) slope means westerly (easterly) anomalies dominate in the region during that month. Although the top panel of **Figure 8** shows a variety of cumulative ZWA evolutions for all ENSO cases, in particular the EPEN and CPEN cases separate very well, while the HBEN cases overlap with both types. The composites in the bottom panel of **Figure 8** capture the distinctive ZWA behaviors for each ENSO type. For the EPEN, strong and continuous westerly wind anomalies are observed, especially in the period of Feb(0) to Nov(0) as shown by the steeper positive slope. For the CPEN, there are weak westerly ZWA over the western most Pacific, because of easterly wind anomalies east of 160ºE leading to a zonal wind convergence to the west of 160ºE as discussed later and shown in **Figure 9**. The ZWA for HBEN falls between the two, with westerly anomalies starting from Apr(0) to

Dec(0). Interestingly, the two most recent HB events of 2006/07 and 2009/10 are different. They show net easterly wind anomalies throughout the evolution of the events with only a short period of westerly wind anomalies evolving in mid to late summer as shown by the positive slopes in **Figure 8**. This means there appears to be only a short period of time suitable for triggering weak Kelvin waves. We discuss this further in the final section.

Figure 9 displays the composites of the temporal patterns of ZWA in shadings, overlaid by the SSTA in contours to further examine the air-sea interactions, for the three types of EN. The small number of events prevents a meaningful statistical analysis. So, these figures should be taken as a qualitative indication of the underlying processes. For EPEN ZWA, the westerly anomalies dominate most of the WP-CP region and extend to the EP boundary (90ºW) in Feb(1). Initially, a CPEN-like SSTA pattern appears briefly in Jan(0)-Feb(0) with a zonal wind convergence over the CP and positive SSTA occurring at the eastern edge of the westerly wind anomalies. Soon after Feb(0), strong westerly wind anomalies occur, triggering a Kelvin wave (**Figure 3a**). Propagation of the Kelvin wave starts when the SSTA is still dominated by the CPEN zonal feedback and surface convergence mechanism. As a consequence, positive SSTA reach the EP in Apr(0). The easterly wind anomalies to the East weaken and further retreat to the East Pacific. Subsequent westerly wind bursts continue to trigger Kelvin waves (**Figure 3a**). When these Kelvin waves reach the easternmost equatorial Pacific, a strong thermocline feedback causes a strong EP warming.

In the case of CPEN, the westerly ZWA remain confined to the WP around 120ºE-160ºE. At the same time, there are easterly anomalies over the EP from about 170ºE to 90ºW (mid panel, **Figure 9**). This means that near-surface convergence in atmosphere and ocean leads to a localised warming over the western CP. The positive SSTA are restricted to the region near the East of the westerly wind anomalies. Over this region the background easterly wind is reduced resulting in enhanced SST due to reduced turbulent heat fluxes and reduced vertical oceanic turbulent mixing (Kug et al., 2009).

All the individual cases of HBEN behave differently (**Figures 5 and 8**), but the key difference to EPEN is that in the mean the westerly wind anomalies remain over the western-most warm pool region until May(0). The initial state of HBEN resembles that of the CPEN, with convergence and positive SSTA near 150ºE. Compared to the EPEN case, the westerly wind anomalies are weaker and do not extend as far into the CP. The CP warming pattern favours deep convection over the higher SST. This intensifies the low-level westerly wind anomalies in the western-central Pacific region. The westerly anomalies gradually extend into the CP region like in the EPEN. At the end of boreal summer, the westerly wind anomalies are strong enough to trigger an additional, stronger Kelvin wave (**Figure 3c**). When this wave reaches the EP boundary, the thermocline feedback leads to positive SSTA.

Hence, in addition to the importance of the WP recharged state, westerly wind anomalies during boreal spring to summer are important for the ENSO development later in the year. For example, the 1982-83 EPEN and 1986-87 HBEN had similar recharged state but evolved differently because westerly wind anomalies were different. For the EPEN 1982-83, westerly ZWA were observed early in the year around April 1982, causing strong downwelling, accumulating the upper ocean heat content. During the evolution of the 1986-87 HBEN westerly wind anomalies remained weak and did not strengthen until Oct 1986 (**Figure 8**). The anomalously strong WP recharged state in both 2006-07 and 2009-10 not resulting in an EPEN event can now be explained using top panel of **Figure 8**. The two factors that determine the strength of an EN event are the western Pacific recharged state and the western-central Pacific cumulative ZWA. Although the initial states in both events were strongly recharged, only weak cumulative ZWA were observed, and the excited Kelvin waves were only weak. After 1997-98 EPEN, Pacific trade winds were strong (Hong et al. 2013; England et al. 2014), and this impeded any process creating westerly wind anomalies.

The cumulative ZWA up to the time of the maximum SSTA explains approximately 60% of the total variance for the maximum SSTA in Niño3.4, Niño3, and Niño1+2. The SSTA over the central-eastern Pacific is affected by the thermocline feedback. The thermocline feedback relates to the propagation of Kelvin waves and

requires strong and continuous westerly wind anomalies along the equator. Hence, the SSTA of Nino1+2 depends more on the westerly wind anomalies than other Niño regions. For the Nino4 region the thermocline feedback is weak so that there is no correlation between maximum SSTA and cumulative ZWA.

3.5 Combined effects of zonal wind anomalies and thermocline state

Both, cumulative ZWA and PTA can explain some variance of maximum SSTA during ENs. We now investigate the combined effect of initial recharged state (θ) and cumulative ZWA (U). For simplicity, we consider the Western Pacific thermocline recharge-discharge state together with the cumulative ZWA as a linear combination of both effects. The Western Pacific mean PTA during Feb(0) from **Figure 6** is used to describe the initial recharged state θ. We calculate the expected maximum SSTA, $\langle T \rangle$, using the following equation,

$$\langle T \rangle = \alpha \cdot \theta + \beta \cdot U \quad (1)$$

Coefficients α and β are multiplied to θ and U, respectively. β has units of Kelvin per ms^{-1}. $\beta \cdot U$ describes the combined effects of thermocline feedback, zonal advection, and heat flux due to zonal wind forcing on SST. The values of α and β are chosen so that R^2 is maximized and the bias of $\langle T \rangle - T_{max}$ minimized. The result for Nino4 is not shown because the correlation is still weak since equation (1) is mainly relevant for mechanisms related to Kelvin wave propagation.

Figure 10 shows the close linear relation between expected and observed maximum SSTA ($\langle T \rangle$ and T_{max}) when information over the full evolution is taken into account for the ZWA, i.e. when the ZWA are accumulated up to the time of T_{max}. The explained variances for the three regions are all above 80% (compared to only 60% when only ZWA is considered). This confirms that the strength of an EN event is highly dependent on two factors: cumulative (or sustained) westerly wind anomalies and the WP recharged state.

The ratio of β to α is larger for Niño1+2 (0.122) than for Niño3 (0.106) and Niño3.4 (0.103). This indicates that the contribution from the westerly wind anomalies in warming Niño1+2 is stronger than in warming the Niño3 and Niño3.4. The Kelvin wave can more easily propagate to Niño3 and Niño3.4 without much dissipation. However, in Nino1+2, winds become more important because a complete eastward propagation of a Kelvin wave to the eastern-most Pacific has to be sustained by continuous westerly wind anomalies.

Generally, an EPEN will occur if the two factors are strong and superimposed constructively. For CPEN, both factors are weak and therefore the thermocline feedback mechanism is not active, leaving only the effects of localized air-sea interactions and zonal advection feedback to sustain the CP warming. The level of constructive or non-constructive superpositions of both factors will result in a range of strengths for the EN events, which is the EN continuum, with CPEN and EPEN as end members.

4. Discussions and Conclusions

By analysing the temporal and spatial SSTA evolutions of EN events, we find that all events start with CP warming patterns. Initially, there are westerly wind anomalies around 120ºE-150ºE and easterly wind anomalies around or east of 180º. This allows eastward extension of the WP warm pool into the CP, but the warm sea surface water is confined by the easterly winds. This localised air-sea interaction is maintained by convective activity in the atmosphere.

We also find that each individual event evolved fairly differently. The 1982-83 and 1997-98 EPEN can be explained well by the recharge-discharge oscillator and delayed oscillator theory (Suarez and Schopf 1988; Battisti and Hirst 1989; Jin 1997). These events involve major Kelvin waves that fully propagate to the eastern-

most Pacific and induce strong SSTA through the thermocline feedback. The 2003-04 and 2004-05 events had SSTA only confined in the CP. All the rest of the events had SSTA spatial patterns and intensities that lie in between CPEN and EPEN.

We found two parameters that determine the evolution of the events and confirm the "El Niño continuum" described by Giese and Ray (2011): the Feb(0) western Pacific recharged state as measured by PTA and the western-central Pacific cumulative ZWA. Both are related to the Kelvin wave mechanisms, and therefore the thermocline feedback. Using these two parameters, we are able to explain more than 80% variability of the maximum SSTA in all the standard Niño regions, except Niño4 because there the thermocline feedback is not important. This shows that the thermocline feedback and the initial recharged state of the WP and winds are equally important. A recharged state alone is necessary but not sufficient for the development of an EN event. The CPEN and EPEN are the end members of the El Niño continuum.

Fedorov et al. (2014) and Hu et al. (2014) used models to explore how different ocean recharged states forced with prescribed one-month WWB affect the diversity of EN flavours. They reach similar conclusions as we have found based on observations. Thus, our results support previous hypotheses. In addition, we proved that cumulative ZWA are more important in determining the EN evolution than a single one-month WWB. With our analysis using a longer period of observational data than Meinen and McPhaden (2000), we are also able to explain the EN evolution after the Pacific climate regime shift (Hong et al. 2013).

In the case of EPEN, the WP recharged state is needed for a Kelvin wave to be triggered. Strong continuous westerly anomalies initiate and sustain the eastward propagation of Kelvin waves to the eastern-most Pacific region. Both factors superimpose constructively in the thermocline feedback mechanism. The HBENs fill in the El Niño continuum whereby the two parameters contribute differently for each of these events. Either the WP is moderately recharged with only moderate westerly wind anomalies, or the WP is strongly (weakly) recharged but with a weak (strong) westerly wind anomaly. Hence, a fully-fledged EPEN event is suppressed.

With these two parameters, we are now able to explain why only after the 2000s there are two pure CP warming events (2003-04, 2004-05), and two events with strong WP recharged states that have not developed into a fully-fledged EPEN (2006-07, 2009-10). This is mainly due to the recent rapid Indian Ocean warming (Rao et al. 2011), which strengthened easterly trade winds and Walker circulation in the past two decades (England et al. 2014). McGregor et al. (2014) also demonstrated that the unusual warming of the North Atlantic contributed strongly to the intensification of the Pacific Walker circulation. The easterly winds prevent Kelvin waves to fully propagate to the eastern-most Pacific and EP warming is suppressed by EP upwelling due to the intensified easterly winds.

In addition, evidence in our study (e.g. Table 1) suggests that there is a transition in the EN evolution after the 1997. As mentioned in the introduction, the phase of the NPO could play a role in the EN diversity observed, but NPO alone is not sufficient to explain the range of EN types. The transition to EN events characterized by CP warming patterns is related to the Pacific climate regime shift (Hong et al. 2013) including the effect of increased easterly winds. In the early 2000s, when the trade winds started strengthening, the WP was not at a recharged state due to the previous strong 1997-98 EPEN event. During the regime shift, the 2002-03 HBEN started off with a relatively weak recharged state. The moderate westerly wind anomalies led to a moderate event. As the background climate state entered a new phase, WP westerly wind anomalies on top of the increased trade wind only permitted localised CP warming, and led to the 2003-04 and 2004-05 CPEN events.

With the continuous easterly winds, warm water gradually accumulated in the WP so that the Pacific warm pool region was highly recharged by early 2006 (**top panel, Figure 5**). The fact that the warm pool was recharged further to the west (between 120 and 140^{o}E) in 2006-07 and 2009-10 compared to previous EN events means that westerly wind anomalies occurring further to the west, approximately 120ºE-130ºE (not shown) were responsible for the initial Kelvin wave of these events. So, the 140ºE-160ºW region that we use in this study in zonal wind analysis does not fully capture the initiation of these events. This has led to an underestimation of

542 the expected maximum SSTA for the 2009-10 event by equation (1). In 2006-07 and 2009-10, slackening of the strong easterly wind anomalies was sufficient to trigger a Kelvin wave. The effect of a weakening of the easterly
544 wind anomalies compared to climatological values is comparable to the effect of westerly wind anomalies triggering a Kelvin wave. Considering the reduction of easterly wind over the western-central Pacific rather than
546 anomalies from the climatology before and at the EN onset is possibly an even more efficient way of determining the evolution of EN.

548 A number of studies using climate models have suggested that there would be more EPEN events under global warming (e.g. Kim and Yu 2012, Santoso et al. 2013; Cai et al. 2014). Our results seem to
550 contradict this. The main reason is that these models fail to reproduce the observed warming of the Indian and Atlantic Oceans, and therefore fail to reproduce the strengthened easterly trade winds (Grose et al. 2014). As
552 long as these strong easterly winds continue, a strong EPEN is not likely to occur.

Forecasting of the maximum SST warming based on the two key parameters PTA and cumulative
554 ZWA is possible. A preliminary trial was done by plotting T_{max} against $\langle T \rangle$ (equation 1) for times before the occurrence of maximum SSTA. For the cumulative ZWA in Jul(0), i.e. six months before the maximum SSTA,
556 we were able to explain 84% of the variability for Niño3. The potential for EN forecasting is promising, and will be covered in a publication in the near future.

558

References

An, S.-I., & Jin, F.-F. (2001). Collective Role of Thermocline and Zonal Advective Feedbacks in the ENSO Mode. *Journal of Climate*, *14*, 3421–3432.

Angell, J. K. (1981). Comparison of variations in atmospheric quantities with sea surface temperature variations in equatorial eastern Pacific.pdf. *Monthly Weather Review*, *109*, 230–243.

Ashok, K., Behera, S. K., Rao, S. a., Weng, H., & Yamagata, T. (2007). El Niño Modoki and its possible teleconnection. *Journal of Geophysical Research*, *112*(C11), C11007. doi:10.1029/2006JC003798

Behringer, D., & Xue, Y. (2004). Evaluation of the global ocean data assimilation system at NCEP: the Pacific Ocean. *Eighth Symposium on Integrated Observing and Assimilation Systems for Atmosphere, Oceans, and Land Surface, AMS 84th Annual Meeting, Washington State Convention and Trade Center, Seattle, Washington*, (January), 11–15.

Bergman, J. W., Hendon, H. H., & Weickmann, K. M. (2001). Intraseasonal Air–Sea Interactions at the Onset of El Nino. *Journal of Climate*, *14*, 1702–1719.

Bjerknes, J. (1966). A possible response of the atmospheric Hadley circulation to equatorial anomalies of ocean temperature. *Tellus*, *18*, 820–829.

C.S. Meinen, M. J. M. (2000). Observations of Warm Water Volume Changes in the Equatorial Pacific and Their Relationship to El Nino and La Nina. *Journal of Climate*, *13*, 3551–3559. doi:10.1175/1520-0442(2000)013<3551:OOWWVC>2.0.CO;2

Cai, W., Borlace, S., Lengaigne, M., van Rensch, P., Collins, M., Vecchi, G., … Jin, F.-F. (2014). Increasing frequency of extreme El Niño events due to greenhouse warming. *Nature Climate Change*, *4*(2), 111–116. doi:10.1038/nclimate2100

Chen, D., Cane, M. a, Kaplan, A., Zebiak, S. E., & Huang, D. (2004). Predictability of El Niño over the past 148 years. *Nature*, *428*(6984), 733–6. doi:10.1038/nature02439

Chen, S., Chen, W., Yu, B., & Graf, H.-F. (2013). Modulation of the seasonal footprinting mechanism by the boreal spring Arctic Oscillation. *Geophysical Research Letters*, *40*(November), n/a–n/a. doi:10.1002/2013GL058628

Compo, G. P., Whitaker, J. S., Sardeshmukh, P. D., Matsui, N., Allan, R. J., Yin, X., … Worley, S. J. (2011). The Twentieth Century Reanalysis Project. *Quarterly Journal of the Royal Meteorological Society*, *137*(654), 1–28. doi:10.1002/qj.776

England, M. H., Mcgregor, S., Spence, P., Meehl, G. A., Timmermann, A., Cai, W., … Santoso, A. (2014). Recent intensification of wind-driven circulation in the Pacific and the Ongoing Warming Hiatus. *Nature Climate Change*, *4*(February). doi:10.1038/NCLIMATE2106

Fedorov, A. V. (2002). The response of the coupled tropical ocean-atmosphere to westerly wind bursts. *Quarterly Journal of Royal Meteorological Society*, *128*, 1–23.

Fedorov, A. V., Hu, S., Lengaigne, M., & Guilyardi, E. (2014). The impact of westerly wind bursts and ocean initial state on the development, and diversity of El Niño events. *Climate Dynamics*. doi:10.1007/s00382-014-2126-4

Giese, B. S., & Ray, S. (2011). El Niño variability in simple ocean data assimilation (SODA), 1871–2008. *Journal of Geophysical Research*, *116*(C2), C02024. doi:10.1029/2010JC006695

Graf, H.-F. (1986). El-Nino Southern Oscillation and Northern Hemispheric Temperature. *Gerlands Beitr. Geophysik*, *1*, 63–75.

598 Graf, H.-F., & Zanchettin, D. (2012). Central Pacific El Niño, the "subtropical bridge," and Eurasian climate. *Journal of Geophysical Research*, *117*(D1), D01102. doi:10.1029/2011JD016493

600 Grose, M. R., Brown, J. N., Narsey, S., Brown, J. R., Murphy, B. F., Langlais, C., … Irving, D. B. (2014). Assessment of the CMIP5 global climate model simulations of the western tropical Pacific climate system and comparison to CMIP3.
602 *International Journal of Climatology*, *34*(February), 3382–3399. doi:10.1002/joc.3916

Hong, C.-C., Wu, Y.-K., Li, T., & Chang, C.-C. (2013). The climate regime shift over the Pacific during 1996/1997. *Climate*
604 *Dynamics*, *43*(1-2), 435–446. doi:10.1007/s00382-013-1867-9

Hu, S., Fedorov, A. V., Lengaigne, M., & Guilyardi, E. (2014). The impact of westerly wind bursts on the diversity and
606 predictability of El Niño events: An ocean energetics perspective. *Geophysical Research Letters*, *41*, 4654–4663. doi:10.1002/2013GL058954.Received

608 Jin, F., & An, S. (1999). Within the Equatorial Ocean Recharge Oscillator Model for ENSO. *Geophysical Research Letters*, *26*(19), 2989–2992.

610 Jin, F.-F. (1997). An Equatorial Ocean Recharge Paradigm for ENSO . Part I : Conceptual Model. *Journal of the Atmospheric Sciences*, *54*, 811–829.

612 Johnson, N. C. (2013). How Many ENSO Flavors Can We Distinguish? *Journal of Climate*, *26*(13), 4816–4827. doi:10.1175/JCLI-D-12-00649.1

614 Kao, H.-Y., & Yu, J.-Y. (2009). Contrasting Eastern-Pacific and Central-Pacific Types of ENSO. *Journal of Climate*, *22*(3), 615–632. doi:10.1175/2008JCLI2309.1

616 Kessler, W. S. (2002). Is ENSO a cycle or a series of events? *Geophysical Research Letters*, *29*(23), 2125. doi:10.1029/2002GL015924

618 Kim, S. T., & Yu, J.-Y. (2012). The two types of ENSO in CMIP5 models. *Geophysical Research Letters*, *39*(11), n/a–n/a. doi:10.1029/2012GL052006

620 Kim, W., & Cai, W. (2013). The importance of the eastward zonal current for generating extreme El Niño. *Climate Dynamics*, *42*(11-12), 3005–3014. doi:10.1007/s00382-013-1792-y

622 Kug, J.-S., Jin, F.-F., & An, S.-I. (2009). Two Types of El Niño Events: Cold Tongue El Niño and Warm Pool El Niño. *Journal of Climate*, *22*(6), 1499–1515. doi:10.1175/2008JCLI2624.1

624 Lian, T., & Chen, D. (2012). An Evaluation of Rotated EOF Analysis and Its Application to Tropical Pacific SST Variability. *Journal of Climate*, *25*(15), 5361–5373. doi:10.1175/JCLI-D-11-00663.1

626 Mcgregor, S., Timmermann, A., Stuecker, M. F., England, M. H., & Merrifield, M. (2014). Recent Walker circulation strengthening and Pacific cooling amplified by Atlantic warming. *Nature Climate Change*, *4*(October).
628 doi:10.1038/NCLIMATE2330

McPhaden, M. J. (1999). Equatorial waves and the 1997-98 El Nino. *Geophysical Research Letters*, *26*(19), 2961–2964.

630 McPhaden, M. J., Zebiak, S. E., & Glantz, M. H. (2006). ENSO as an integrating concept in earth science. *Science (New York, N.Y.)*, *314*(5806), 1740–5. doi:10.1126/science.1132588

632 Pascolini-Campbell, M., Zanchettin, D., Bothe, O., Timmreck, C., Matei, D., Jungclaus, J. H., & Graf, H.-F. (2014). Toward a record of Central Pacific El Niño events since 1880. *Theoretical and Applied Climatology*. doi:10.1007/s00704-014-
634 1114-2

Rao, S. a., Dhakate, A. R., Saha, S. K., Mahapatra, S., Chaudhari, H. S., Pokhrel, S., & Sahu, S. K. (2011). Why is Indian
636 Ocean warming consistently? *Climatic Change*, *110*(3-4), 709–719. doi:10.1007/s10584-011-0121-x

Reynolds, R. W., Rayner, N. A., Smith, T. M., Stokes, D. C., & Wang, W. (2002). An Improved In Situ and Satellite SST
638 Analysis for Climate. *Journal of Climate*, *15*, 1609–1625.

Santoso, A., McGregor, S., Jin, F.-F., Cai, W., England, M. H., An, S.-I., … Guilyardi, E. (2013). Late-twentieth-century
640 emergence of the El Niño propagation asymmetry and future projections. *Nature*. doi:10.1038/nature12683

Schneider, E. K., Huang, B., & Shukla, J. (1995). Ocean Wave Dynamics and El Nino. *Journal of Climate*.

642 Suarez, M. J., & Schopf, P. S. (1988). A delayed action oscillator for ENSO. *Journal of the Atmospheric Sciences*, *45*, 3283–
3287.

644 Takahashi, K., Montecinos, a., Goubanova, K., & Dewitte, B. (2011). ENSO regimes: Reinterpreting the canonical and
Modoki El Nio. *Geophysical Research Letters*, *38*(May), 1–5. doi:10.1029/2011GL047364

646 Vecchi, G. a, Soden, B. J., Wittenberg, A. T., Held, I. M., Leetmaa, A., & Harrison, M. J. (2006). Weakening of tropical
Pacific atmospheric circulation due to anthropogenic forcing. *Nature*, *441*(7089), 73–6. doi:10.1038/nature04744

648 Yeh, S.-W., Kug, J.-S., & An, S.-I. (2014). Recent progress on two types of El Niño: Observations, dynamics, and future
changes. *Asia-Pacific Journal of Atmospheric Sciences*, *50*(1), 69–81. doi:10.1007/s13143-014-0028-3

650 Yeh, S.-W., Kug, J.-S., Dewitte, B., Kwon, M.-H., Kirtman, B. P., & Jin, F.-F. (2009). El Niño in a changing climate.
Nature, *461*(7263), 511–4. doi:10.1038/nature08316

652 Yu, J.-Y., & Kim, S. T. (2010). Three evolution patterns of Central-Pacific El Niño. *Geophysical Research Letters*, *37*(8),
n/a–n/a. doi:10.1029/2010GL042810

654 Yu, J.-Y., Lu, M.-M., & Kim, S. T. (2012). A change in the relationship between tropical central Pacific SST variability and
the extratropical atmosphere around 1990. *Environmental Research Letters*, *7*(3), 034025. doi:10.1088/1748-
656 9326/7/3/034025

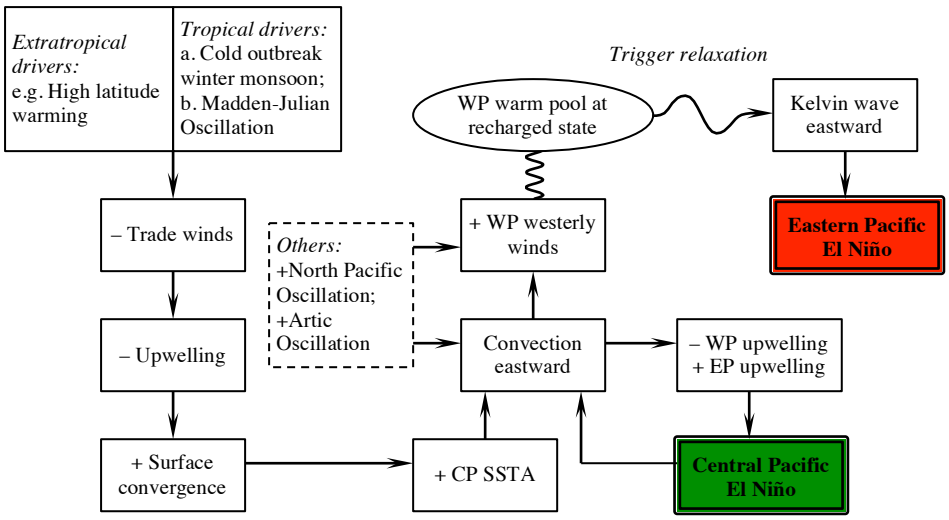

Fig. 1 Slightly amended from Graf (1986), highlighting the causes of Central and Eastern Pacific El Niños. Minus sign denotes decrease; plus sign denotes increase of the parameter under consideration. Dash line box means other drivers, circular box means the parameter already exists within the system

Table 1 Characteristics of El Niño events during 1980-2013

	2009-10	**2006-07**	**2004-05**	**2003-04**	**2002-03**
El Niño type[a]	HB	HB	CP	CP	HB
Evolution Patterns[b]	(CP+EP) ➔ CP	(CP+EP) ➔ CP	CP	CP	CP ➔ EP ➔ CP
Evolution Timeline:					
Onset month[c]	5-2009	6-2006	7-2004	6-2003	7-2001
(CP+EP) or EP Period	5-2009 to 10-2009	7-2006 to 1-2007	NA	NA	11-2002 to 12-2002
Peak month	12-2009	12-2006	11-2004	12-2003	11-2002
Max. SSTA (K)	2.75	2.45	1.82	1.56	2.89
Longitude	105ºW	172ºW	174ºE	168ºE	163ºW
End[d]	4-2010	3-2007	4-2005	2-2004	4-2003

	1997-98	**1994-95**	**1991-92**	**1986-87**	**1982-83**
El Niño type[a]	EP	HB	HB	HB	EP
Evolution Patterns[b]	CP ➔ EP	CP ➔ EP ➔ CP	CP ➔ EP ➔ CP	CP ➔ EP ➔ CP	CP ➔ EP
Evolution Timeline:					
Onset month[c]	3-1997	7-1994	8-1990	8-1986	4-1982
(CP+EP) or EP Period	5-1997 to End	11-1994 to 12-1994	5-1991 to 5-1992	1-1987 to 12-1987	8-1982 to End
Peak month	12-1997	11-1994	4-1992	7-1987	1-1983
Max. SSTA (K)	5.39	2.67	3.25	2.95	5.44
Longitude	106ºW	166ºW	84ºW	156ºW	127ºW
End[d]	5-1998	4-1995	10-1992	2-1988	9-1983

[a] CP, HB, EP = Central Pacific, Hybrid, Eastern Pacific El Niño, respectively

[b] (CP+EP) = CP and EP warming patterns happen simultaneously

[c] Onset = The first month of SSTA ≥ 0.5K occurs in 160ºE-80ºW and 5ºN-5ºS for at least five consecutive months

[d] End = Final month with SSTA ≥ 0.5K inside the region as in "Onset"

(a) Eastern Pacific El Niño

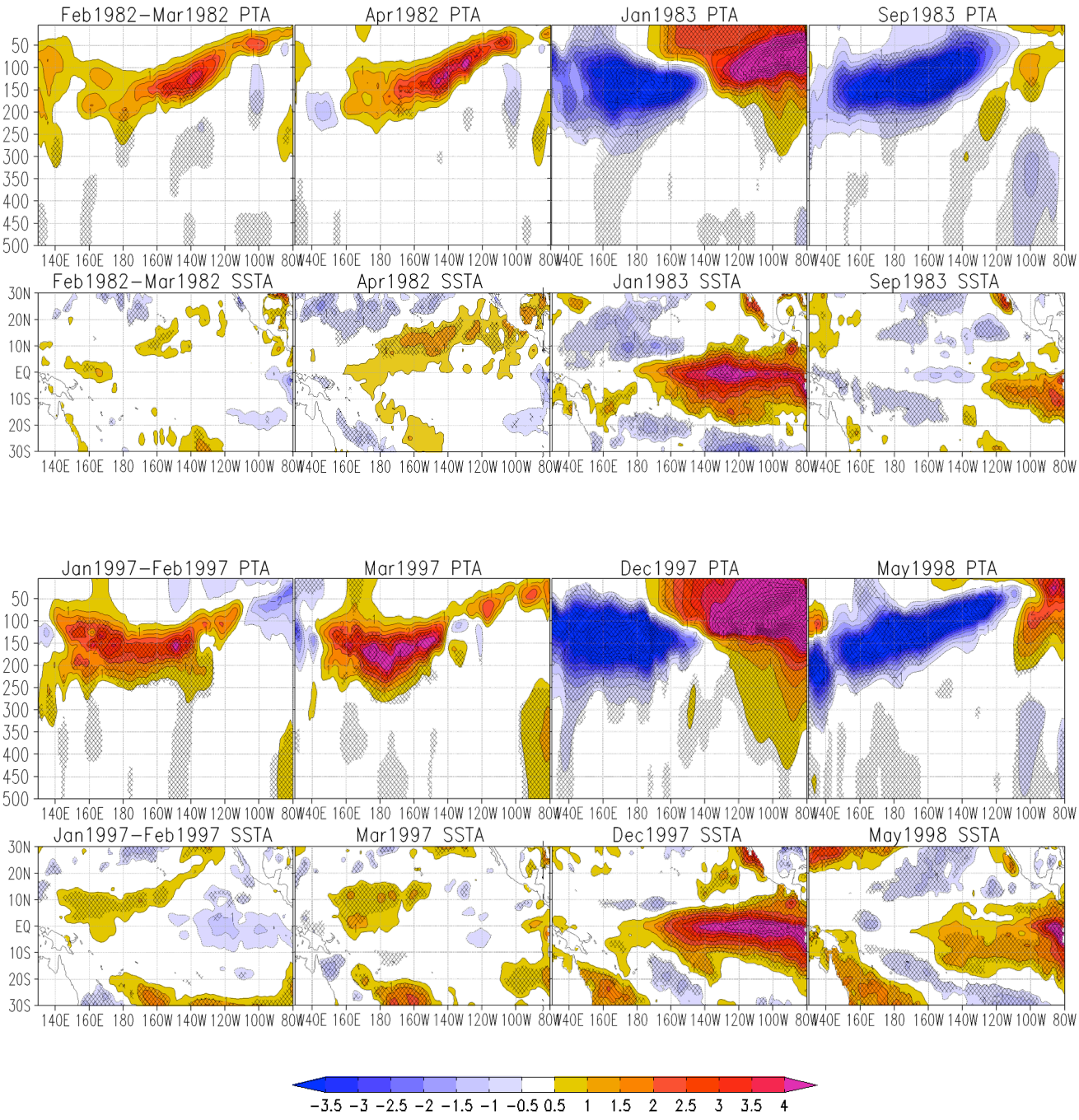

Fig. 2 From left to right panels are the composite of two months before an ENSO onset, the onset month, peak month, and final month, respectively, for **a** EPEN, **b** CPEN, and **c** HBEN. For each ENSO event, the top row shows the 5ºN-5ºS oceanic potential temperature anomalies as a function of depth, the bottom row shows the SSTA. The shading and contours are the anomalies at interval of 0.5ºC. The hatching denotes values that are significant at the 1.3 standard deviations or the 80% confidence level based on a two-tailed z-test.

(b) Central Pacific El Niño

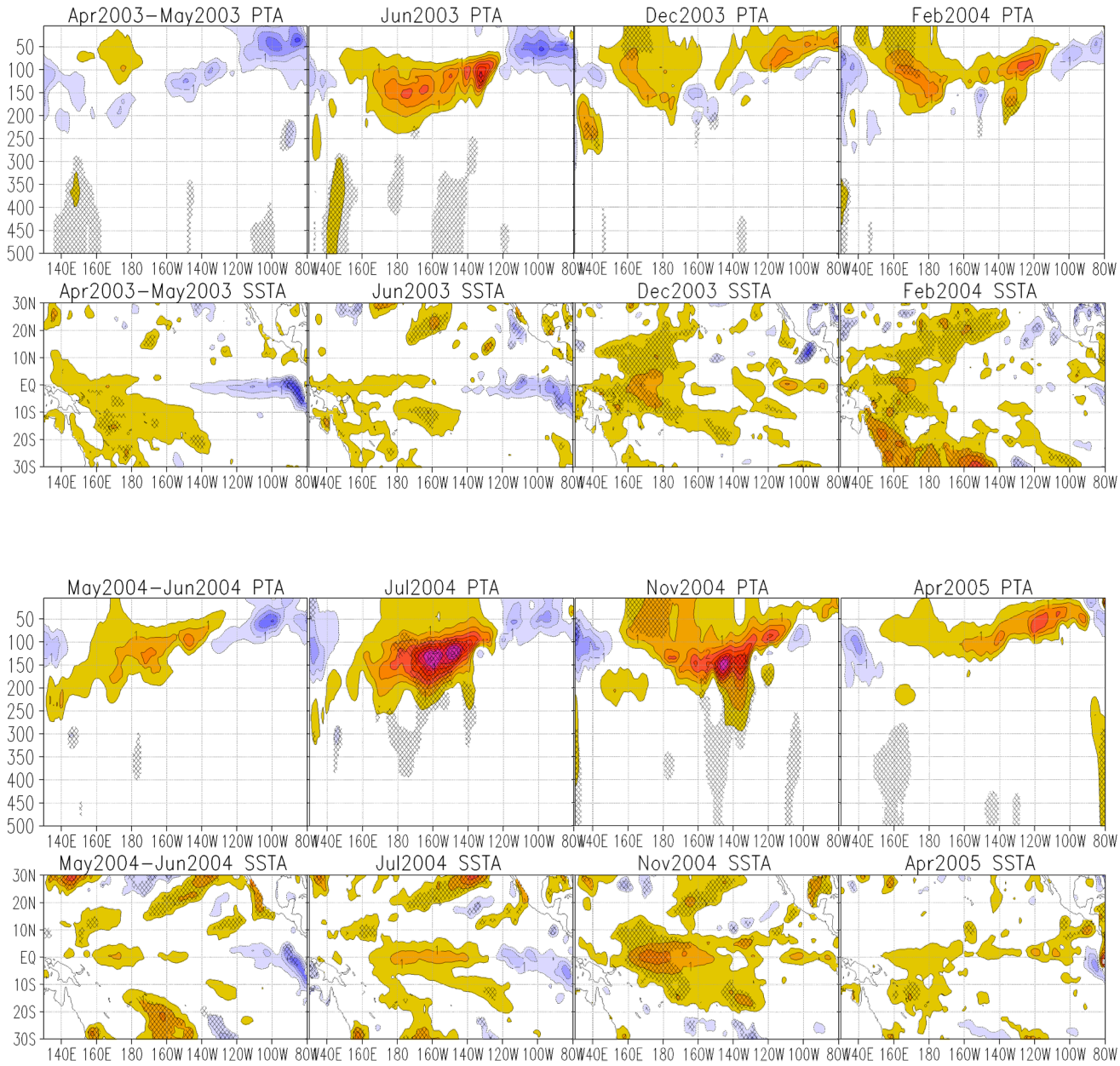

(c) Hybrid El Niño

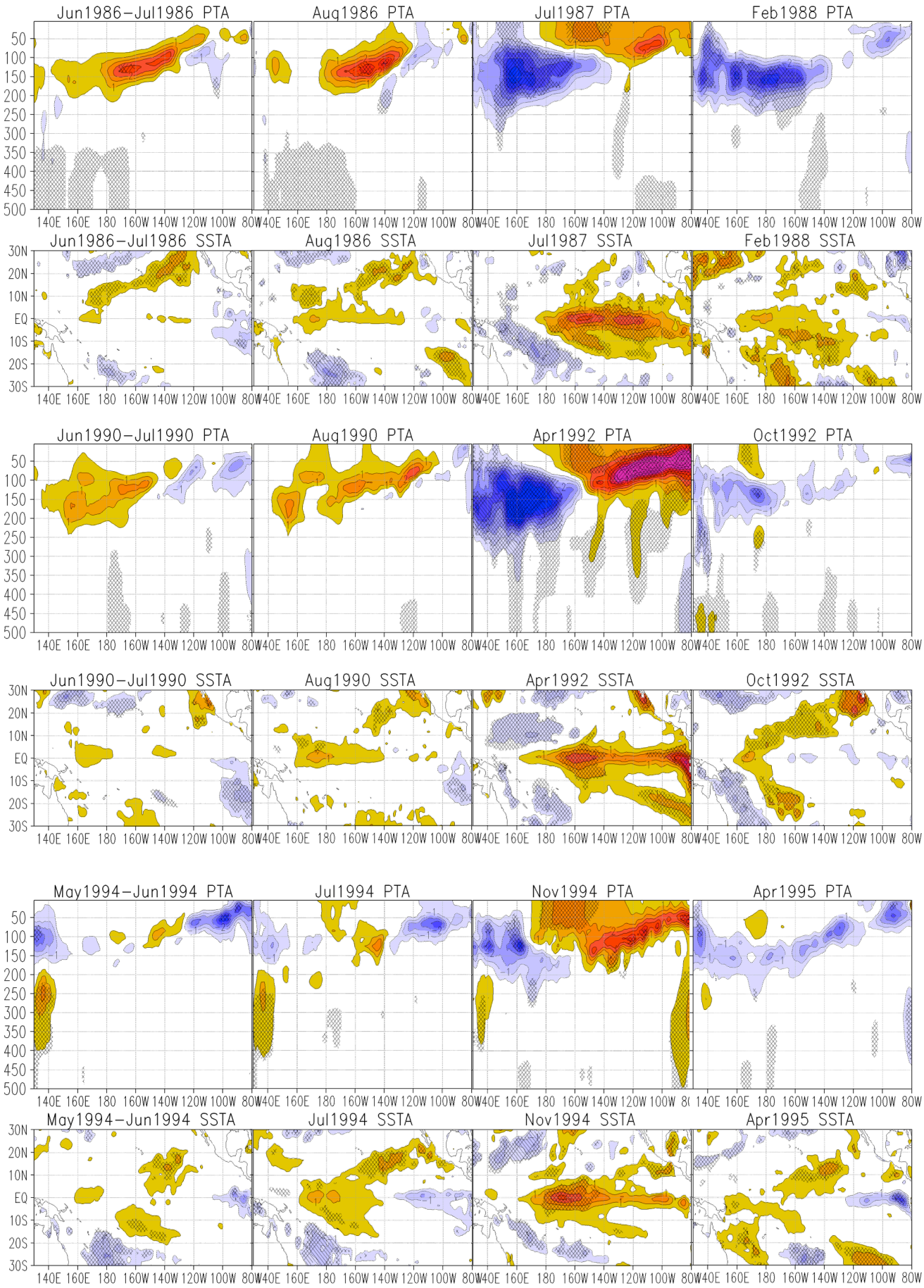

(c) Hybrid El Niño

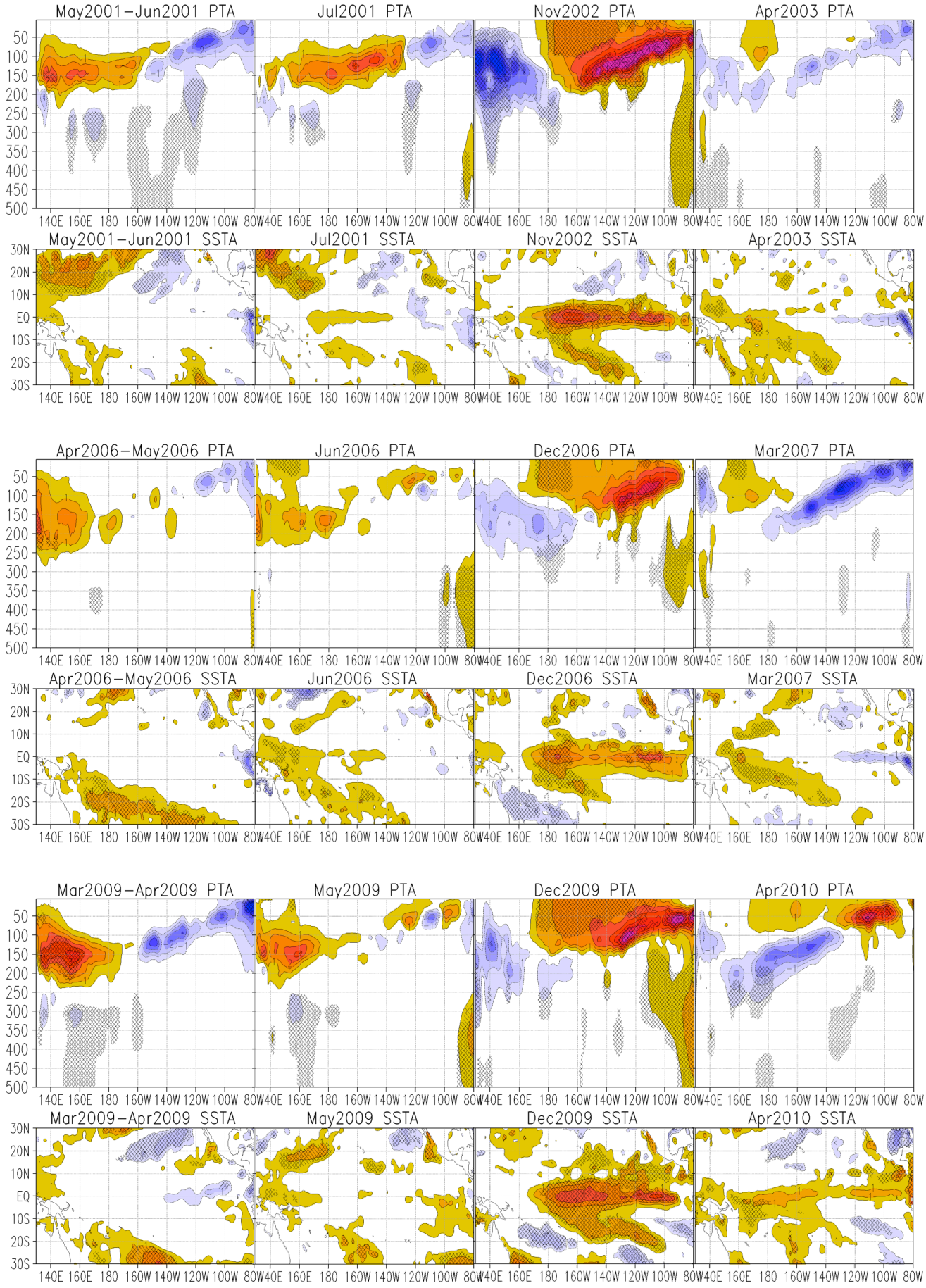

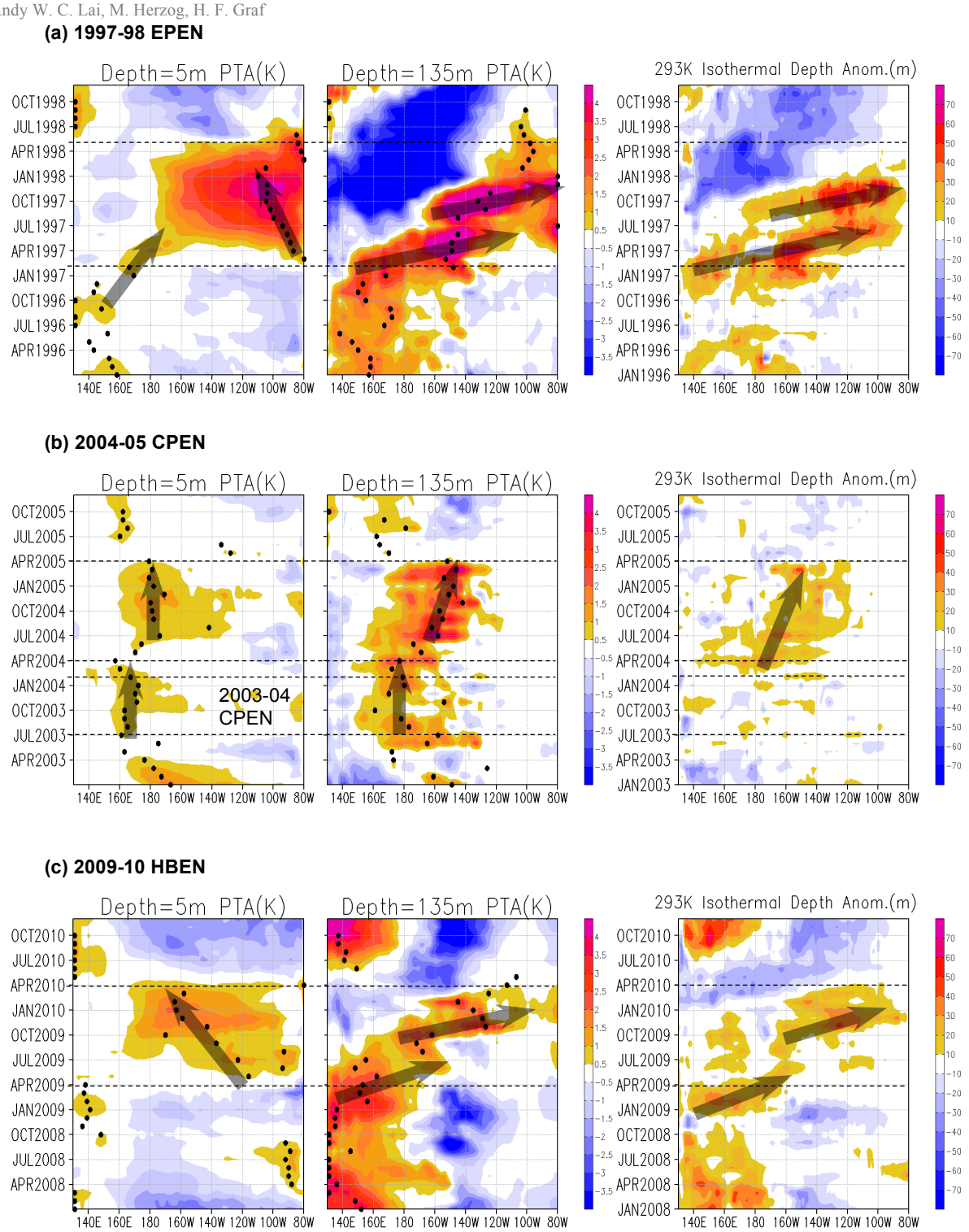

Fig. 3 Oceanic potential temperature on a Hovmoller plots for **a** 1997-98 EPEN, **b** 2004-05 CPEN, **c** 2009-10 HBEN, with left panels at a depth of 5m, middle panels at 105m and right panels for the 293K isothermal depth anomalies. The arrows illustrate the conceptual propagations. The dots denote the maximum potential temperature for each month. The dash lines mark the onset and the final months of the ENSO events.

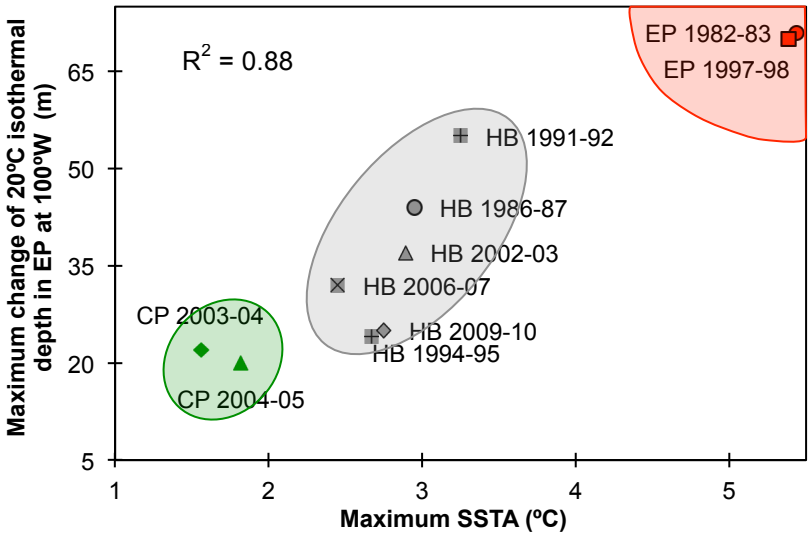

Fig. 4 For each data point shows the maximum SSTA throughout an EN event against the maximum change of the 20ºC isothermal depth over 100ºW during an EN event as defines in **Table 1**. Red, grey, and green denote EPEN, HBEN, and CPEN respectively. The circles show the clustering pattern of the three ENSO types

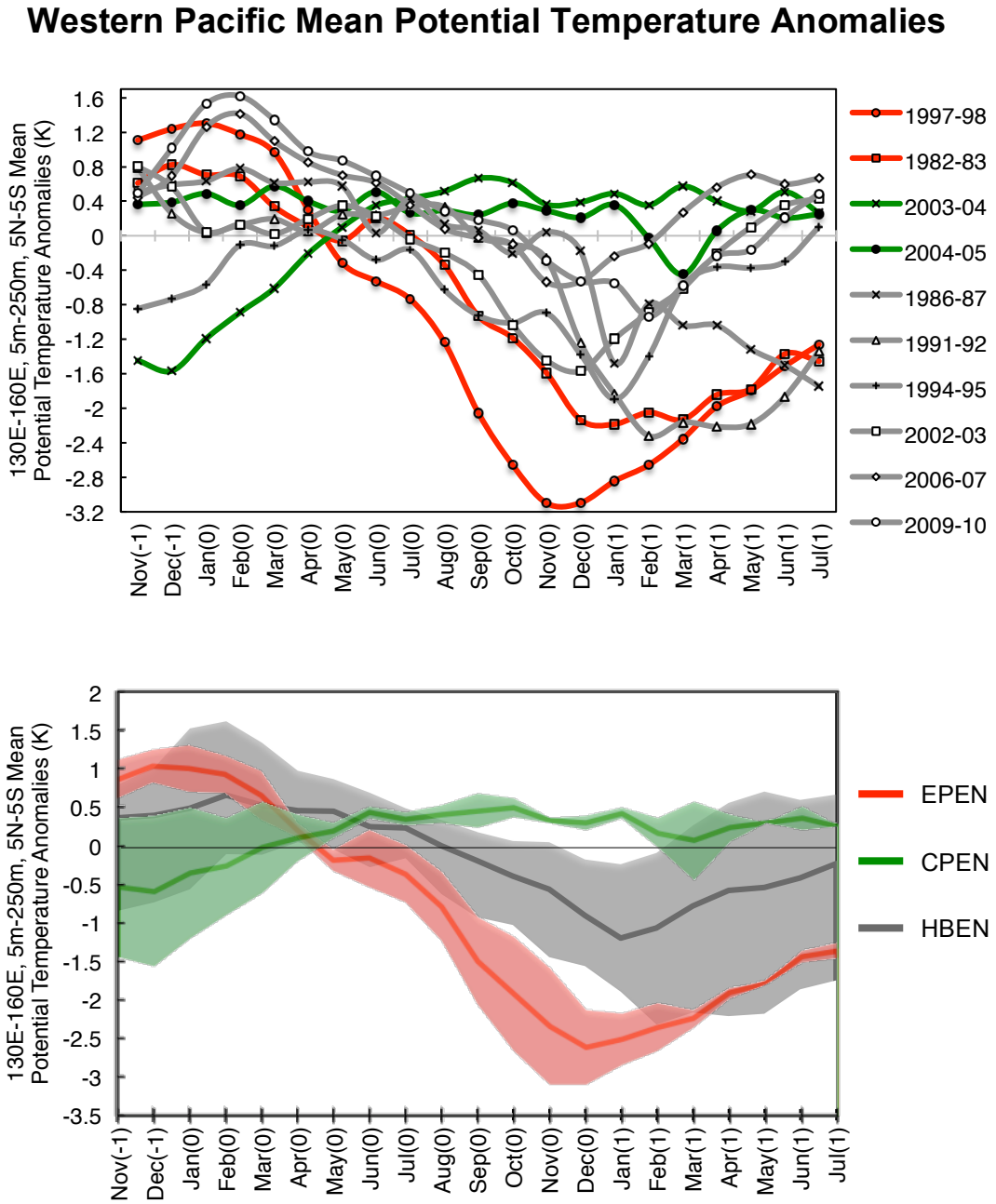

Fig. 5 Mean Western Pacific potential temperature of the volume 130ºE-160ºE, 5ºN-5ºS, and 5m-250m, **top** for all ENSO events during 1980-2013, and **bottom** composite of each ENSO type. Red, grey, and green denote EPEN, HBEN, and CPEN respectively. The shades are the maximum and minimum values in the data of the composites

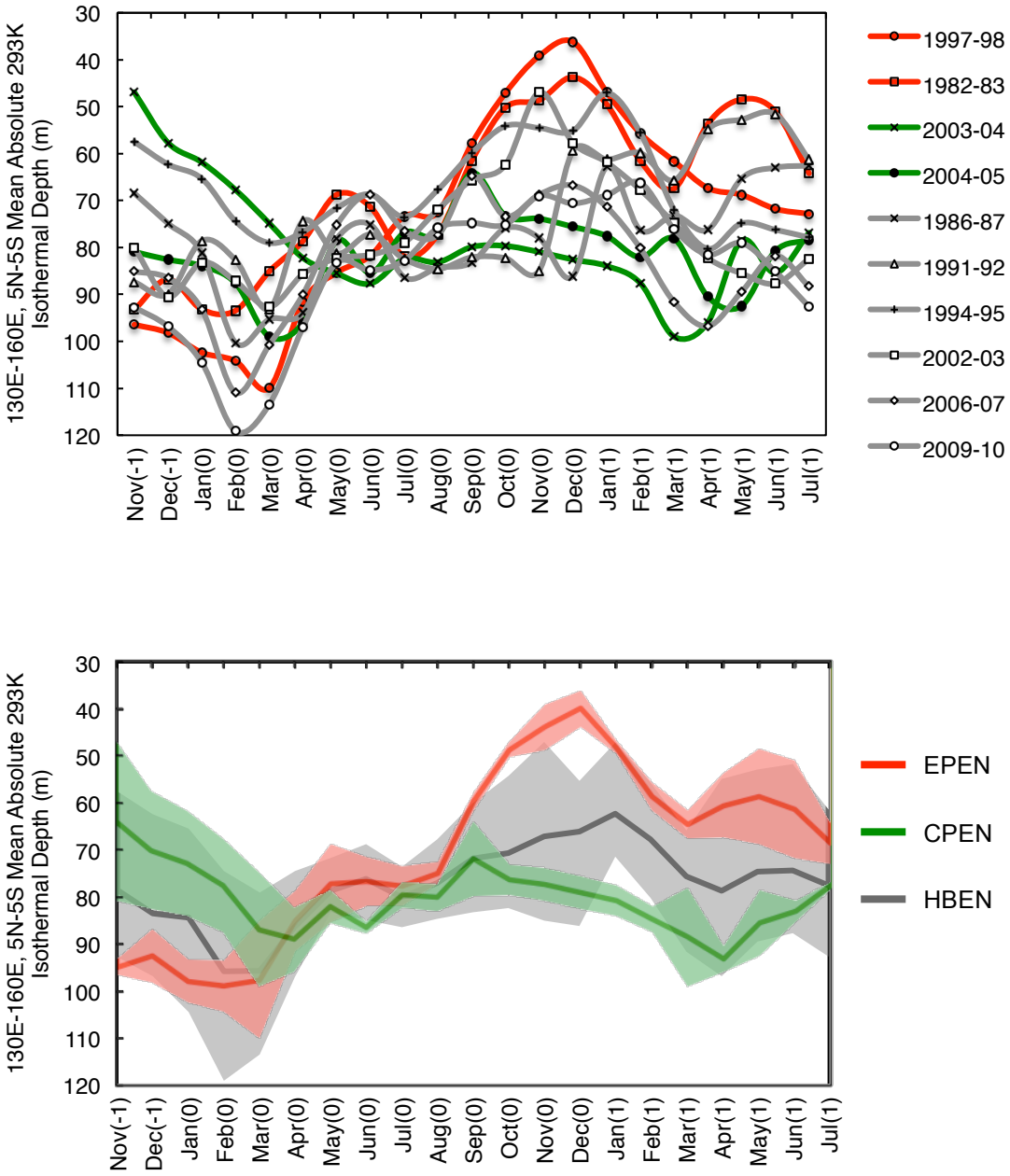

Fig. 6 As in **Fig. 5**, but for the mean absolute 293K isothermal depth over the area 130ºE-160ºE and 5ºN-5ºS

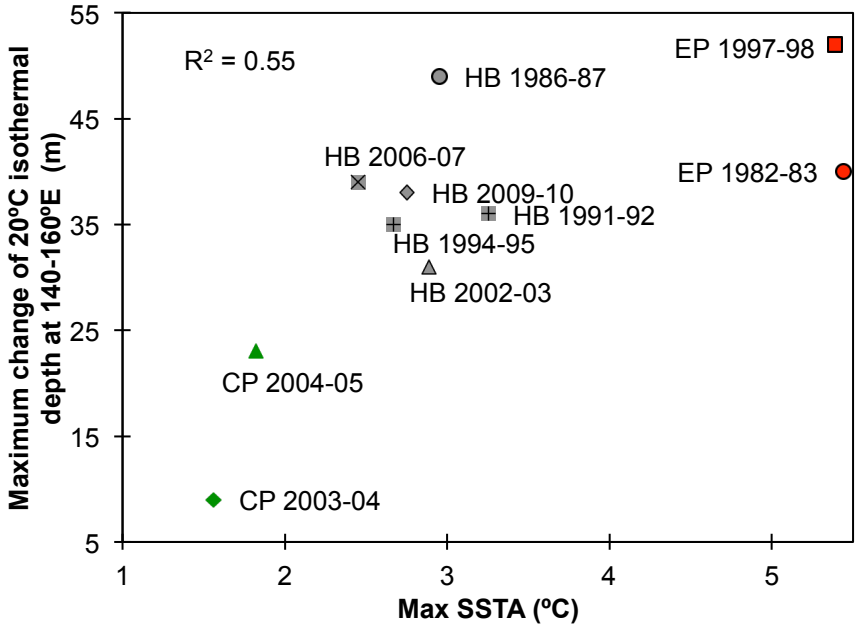

Fig. 7 As in **Fig. 4**, but for 140-160ºE

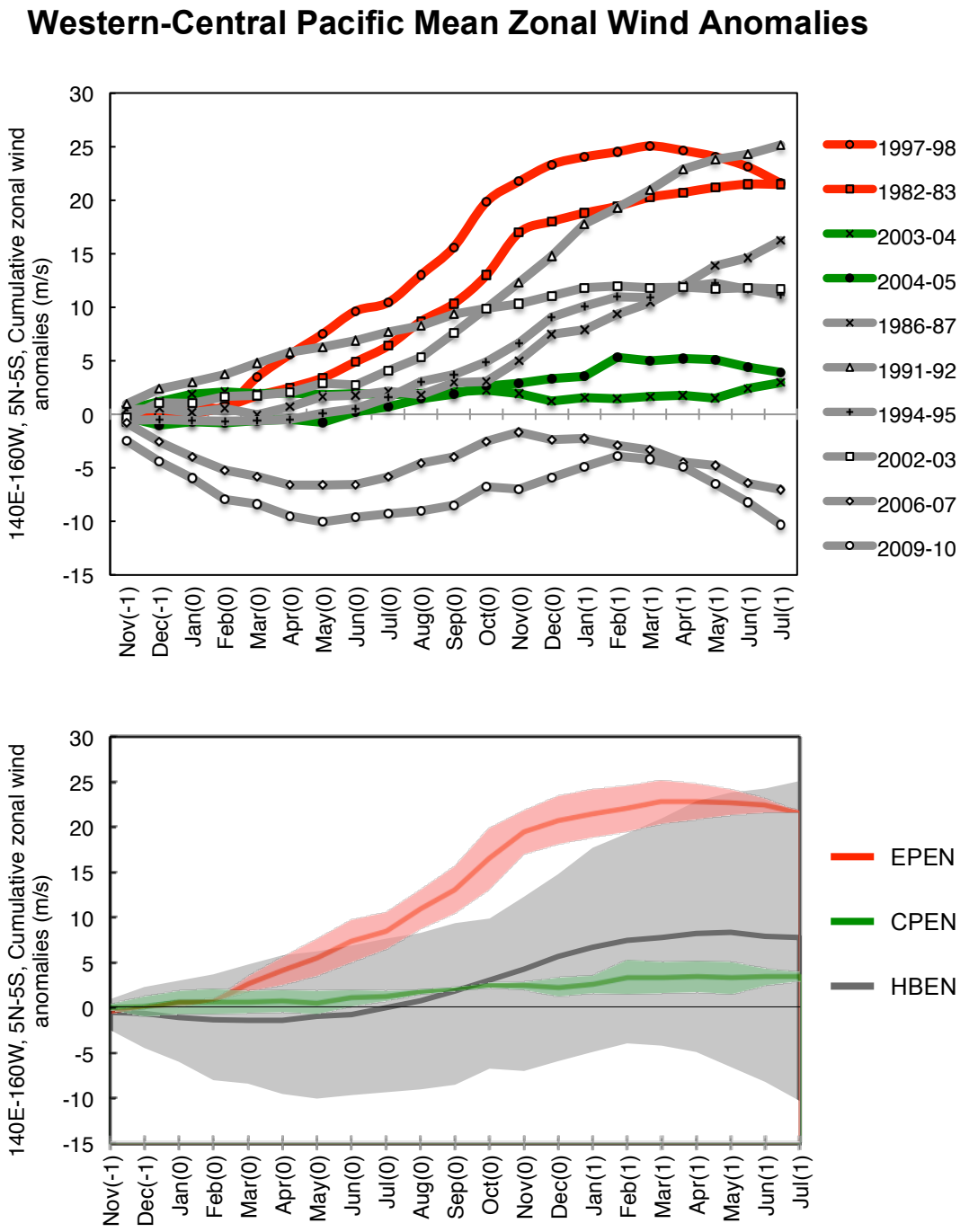

Fig. 8 Western-Central Pacific cumulative zonal wind anomalies of the area 140ºE-160ºW and 5ºN-5ºS **top** for all ENSO events during 1980-2013, and **bottom** composite of each ENSO type. Red, grey, and green denote EPEN, HBEN, and CPEN respectively. The shades are the maximum and minimum values in the data of the composites. Positive anomalies are eastward

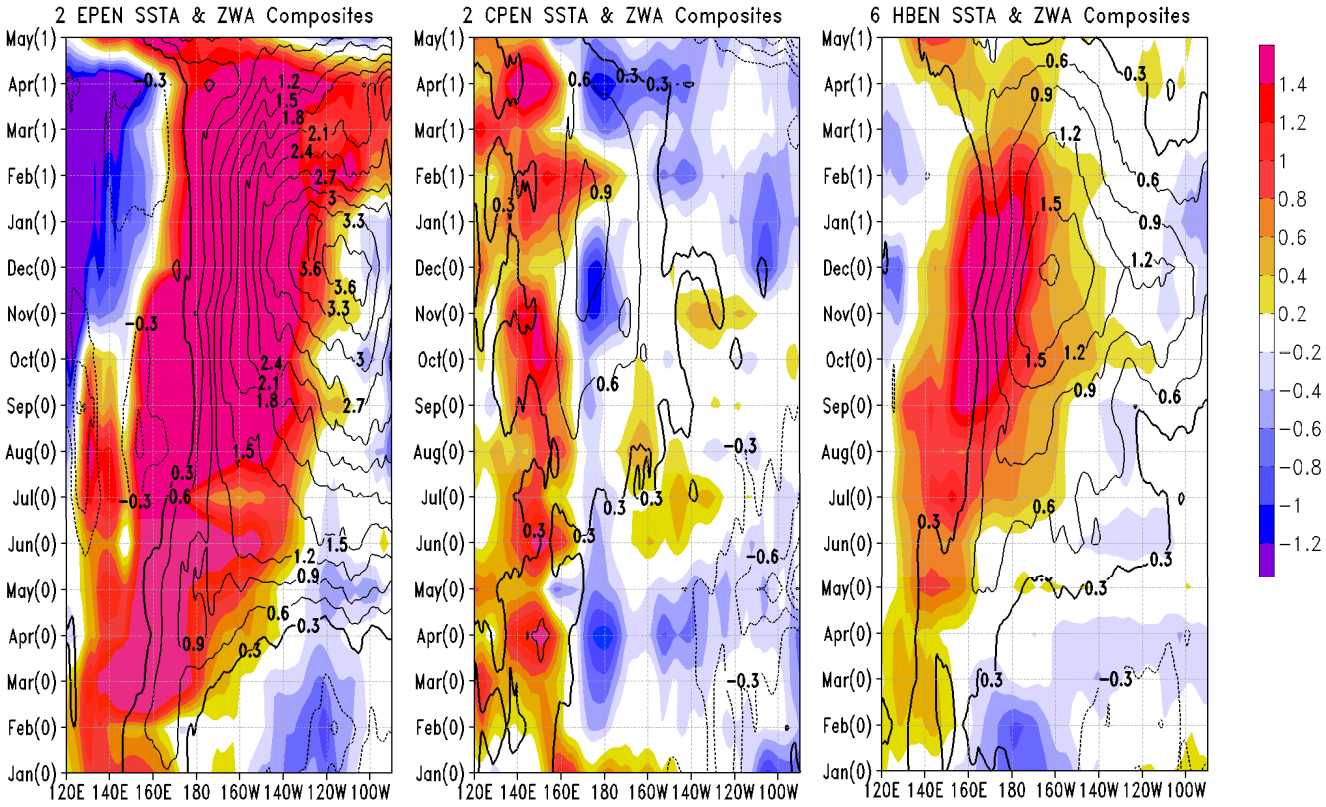

Fig. 9 Zonal wind anomalies (m/s) composites are shaded on Hovmoller plots. SSTA are overlaid in contours at 0.3K intervals. Panels on the left: EPEN, middle: CPEN, and right: HBEN. Positive anomalies are eastward

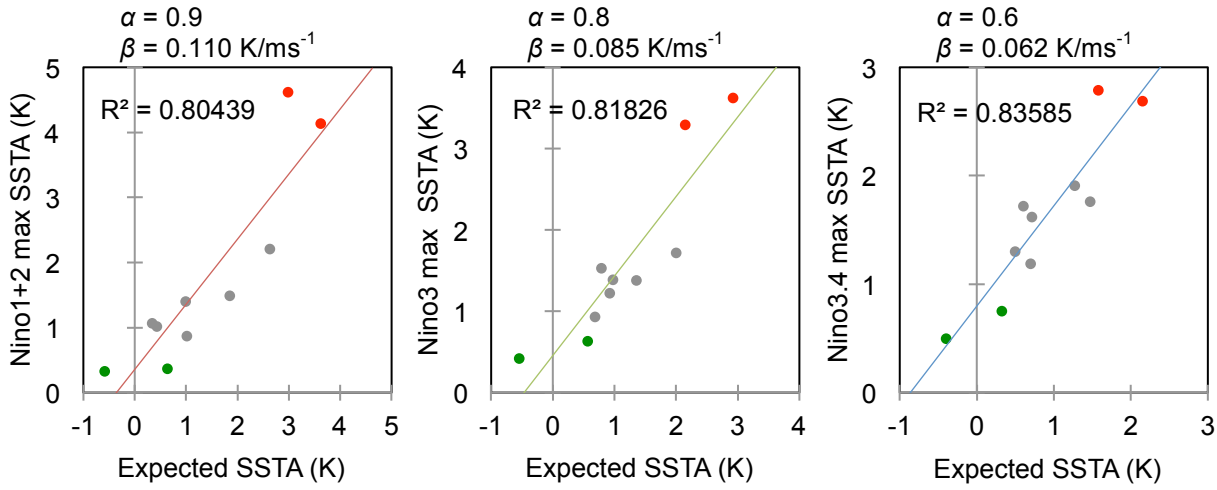

Fig. 10 Linearly adding the Feb(0) PTA (θ) and cumulative ZWA (U) of the month with maximum SSTA with a factor α, and β [K/ms^{-1}] to calculate the expected SSTA $\langle T \rangle = \alpha\theta + \beta U$. This is plotted against the maximum SSTA in: **left** Niño1+2, **middle** Niño3, and **right** Niño3.4